Chinese Chemical Letters 34 (2023) 107694

Contents lists available at ScienceDirect

Chinese Chemical Letters

journal homepage: www.elsevier.com/locate/cclet

Highly efficient synthesis and application of aryl diazonium salts *via* femtosecond laser-tailored 3D flow microfluidic chips

Jing Ren[a], Miao Wu[b], Kaiwu Dong[a], Min Zhang[a], Ya Cheng[b,*], Guoyue Shi[a,*]

[a] *School of Chemistry and Molecular Engineering, Shanghai Key Laboratory for Urban Ecological Processes and Eco-Restoration, East China Normal University, Shanghai 200241, China*
[b] *School of Physics and Electronic Science, East China Normal University, Shanghai 200241, China*

ARTICLE INFO

Article history:
Received 25 May 2022
Revised 13 July 2022
Accepted 18 July 2022
Available online 23 July 2022

Keywords:
3D microfluidic chips
Femtosecond laser micromachining
Flow synthesis
Aryldiazonium salts
Room temperature

ABSTRACT

The first example of the microfluidic chips (MFCs) consisting of centimeter-level 3D channels with high-density and large-volume fabricated by femtosecond laser micromachining were utilized to develop a time-saving, economical and hazardless flow synthesis process, and its advantages have been proved by *in situ* formation of aryldiazonium salts and subsequent borylation with bis(pinacolato)diboron. There are several important advantages in our 3D MFC-based flow synthesis technology, including the following: (1) the reaction temperature was altered from ice bath to room temperature; (2) the residence time was reduced by 10 times; (3) the yield was greatly improved, that is, several arylboronates were successfully obtained with higher yield compared to traditional batch process. Therefore, it can be envisioned that a novel, simplified flow synthetic protocol will be developed toward green organic synthesis *via* MFCs.

Microfluidic chips (MFCs)-involved system seems to be fit naturally as a revolutionary technology in organic synthesis and medicinal chemistry [1,2]. Reaction processes using continuous flow in MFCs for transforming traditional batchwise into manufacturing scales are not without controversy, which have received considerable interest [3]. Flow chemistry endows the MFCs with remarkable capacity to scale those potentially explosive and hazardous reactions due to its precise control of reaction temperature, residence time, high efficient heat transfer and enhanced mass transfer [4,5]. The choice of reactions is broadened to give the anticipated product or intermediate to selections that will not be achieved in traditional flask [6]. Furthermore, MFCs are not only smaller than batch reactors in volume but also can produce greater product in a specified time, so that surpass analogous batch reactors in the ideal setting and optimized conditions [7]. Meanwhile, the production-scale capabilities are achieved by the parallel MFCs and running for longer time without the need for reoptimization, which is also conducive to greener chemistry and a luxury not afforded in batch processes [8].

Since MFCs have gained increasing interests, it is crucial of their material to ensure manufacturing process and application in organic synthesis [9]. Glass shows excellent chemical resistance to most nonpolar or low polar solvents compared to polydimethylsiloxane (PDMS), and has good tolerance for many organic reagents compared to polymethyl methacrylate (PMMA) [10,11]. Thus, such remarkable properties attract us to develop a self-designed glass MFCs with transparency, allowing reactions at high temperatures and pressure, and enabling operators to observe the chemical processes in flow for the organic synthesis [12–14].

Based on some typical glass MFCs technologies, many 2D planar channel shapes for improving fluid mixing have been widely used in the industry, including T-shaped and H-shaped, *etc.* [15,16]. But the fabrication techniques and glass molding process used for these channels are not capable of producing complex 3D structures that can enable more efficiently mixing [17]. Therefore, in order to construct 3D MFCs without stacking and bonding, femtosecond laser micromachining technology, which can perform high-precision spatially-selective modification inside the glass, is introduced [18]. At present, femtosecond laser direct writing applications mostly remained in biomicrochip, of which the length of the mixing channel is usually limited to a few millimetres [19]. Additionally, the ability of MFCs for large-scale chemical applications has been overlooked [20,21]. The processing used in this paper can induce nonlinear absorption (multi-photon absorption) to make strong light absorption of the optical transparent material, and then modify the spatial resolution of the material at nanometer processing scale [22]. With the aid of wet chemical etching, 3D structure micromachining can be completely realized with a di-

* Corresponding authors.
E-mail addresses: ya.cheng@siom.ac.cn (Y. Cheng), gyshi@chem.ecnu.edu.cn (G. Shi).

https://doi.org/10.1016/j.cclet.2022.07.037
1001-8417/

rect and maskless approach [23]. In particular, it has been proved that a 3D structure based on the Baker's transform can provide the highest mixing performance under chaos theory [24]. Our original intention is to demonstrate the ability of 3D MFCs for large-scale chemical applications, as well as to develop a reliable and simple process synthesis tool for green organic synthesis employing MFCs. To the best of our knowledge, this is the first example of the MFCs consisting of such centimeter-level 3D channels with high-density and large-volume are fabricated in Borosilicate glass by femtosecond laser micromachining. A single piece of our chip could realize several 3D chips on the market to have a liquid volume, whereas a single chip on the market was equivalent to the same liquid volume, and its chip was significantly larger than our chip. It represents the functional miniaturization of our equipment, its high integration in the industry, and the fact that our equipment takes up less space, has fewer leaks, and saves a lot of resources. And the high efficiency mixing, mass and heat transfer performance of 3D MFCs are well demonstrated through physical simulation and chemical experiments in this paper.

In our MFCs with 3D configuration, two microfluids were divided along the up-down area and recombined in left and right directions, which eventually split into eight microfluids, and result in seven mass transfer interfaces (Fig. 1a). Accordingly, the slim microfluids could achieve fast and efficient mixing by continuously separating fluid units based on Barker's transform, even at low Reynolds number. To evaluate the mixing intensity, the molar concentration distribution was simulated by solving the microfluidic incompressible Navier-Stokes and convection diffusion equations using computational fluid dynamics (CFD) analysis. The diffusion coefficient of the two kinds of microfluid were set as $1.26 \times 10^{-9}\ m^2/s$. The mixing intensity I_M was defined as follows:

$$I_M = 1 - \sqrt{\frac{\sigma^2}{\sigma_{max}^2}}$$

$$\sigma^2 = \int (c_i - \bar{c})^2 dS$$

S was the section perpendicular to the direction of progress of the fluid, $\bar{c}$ was the optimal mixing concentration, $\bar{c} = 0.5\ mol/m^3$, c_i was the molar concentration at sampling point I on the cross section.

Herein, the study simulated the molar concentration distribution in time and space of the 3D and 2D straight mixing channel ($v = 0.3$ mL/min). Some sophisticated 2D chips used narrowing and extrusion structures to achieve better mixing. But the ensuing pressure drop was considerable, and the chip was readily cracked as a result of this design. This would not only clog chemical applications, but it would also necessitate a lot of driving effort, wasting energy. In mass production, the most typical centimeter-scale channels were coil reactors and T-shaped designs. So we compared our structure to a centimeter-scale 2D Mixer at low Reynolds numbers. The 3D mixing chip was showed in Fig. 1b: the mixing intensity reached 93% after two fluids entered the mixed channel in only 0.78 s, thus achieving perfect mixing. Whereas, the mixing intensity was only 27% in 0.78 s in the 2D mixing chip (Fig. 1c). Thereout, the 3D mixing chip greatly shortened the mixing time, meeting the need for faster chemical reactions and improved chemical synthesis of space-time yield. Then the mixing intensity of two chips was compared at different instants of time at 0.3 mL/min (Fig. S1A in Supporting information). For 3D mixing chips, the mixing intensity increases with residence time, while the mixing process was time-consuming and inefficient in 2D chip without enhanced mixing effect structure. The mixing performance of the 3D MFCs was evidenced by using two kinds of ink in yellow and blue in Fig. 1d ($v = 0.3$ mL/min). In Fig. 1e, the mixing efficiency of 3D mixing chip was compared to 2D mixing chip with the same liquid holding volume ($v = 11.44\ cm^3$), which showed the high mixing efficiency of 3D chip even at low Reynolds number (in inlet). Fig. 1f showed the molar concentration distribution in time and space of the 3D mixing chip, which also evidenced the highly efficient mixing in extremely thin channels or over a wide range of flow speeds was insensitive to Reynolds number through enough mixing units. Meanwhile, in order to investigate the mixing efficiency at various flow rates, similar trends were displayed in Fig. 1g. The reaction solution was completely mixed within 1 s in 3D MFCs in the set flow rate range, which also indicated that the different final yield of the reaction was caused by the time required for chemical reactions rather than mixing.

Table 1
Comparison between traditional reactors and microchannel reactors.

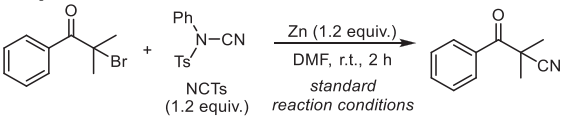

Parameters	Batch	2D mixer	3D MFCs
Temp (°C)	25	60	60
T_1 (min)	N/A	6.87	6.87
T_2 (min)	N/A	7.14	7.14
T (min)	120	14	14
Yield (%)	90	60	100

Encouraged by these simulated results, several studies have demonstrated the benefits of this 3D MFCs in an identical reaction. Treating tertiary alkyl halides and electrophilic cyanation reagents with zinc dust provided a practical and safe route to α-cyano carbonyls [25]. A packed-bed reactor was integrated in a liquid-liquid two-phase continuous flow chemical reaction device, which was filled with zinc metal particles. 2-Bromo-2-methylpropiophe (5.0 mmol) was *in-situ* synthesized into organozinc reagent through the packed bed reactor, and then combined with the electrophilic cyanide reagent *N*-cyano-*N*-phenyl-*p*-toluenesulfonamide (NCTs) (5.0 mmol) in the 3D MFCs to generate α-cyano carbonyl compound (Fig. S5 in Supporting information). Compared with traditional synthesis methods, the optimal reaction parameters in 3D MFCs were as follows: reaction temperature of 60 °C, residence time of 7.14 min, volume flow rate ratio of 2:1 and the yield was 100% (Table 1). The introduction of solid-phase reagents has greatly expanded the application of the 3D MFCs in the synthesis of complex organic compounds, and the device could be easily modified for reactions involving multi-step synthesis, allowing flexible arrangement and on-demand building block synthesis. In the comparative experiment, we replaced the 3D MFCs with a 2D mixer of the same channel size and liquid storage volume, and the other reaction conditions remained unchanged. In the 2D mixer, the yield was only 60% because it did not have the efficient mass transfer of 3D MFCs and could not be stirred as batch reaction. This experiment not only demonstrated the superior performance of the 3D MFCs, but it also enhanced the design concept of the 3D MFCs by displaying the mass transfer effect and temperature difference that numerous mixers presented.

The specific surface area, as a vital factor, of a self-designed microchip of three volumes was calculated compared with that of a half-filled 250 mL round-bottom flask in Table 2. It was clear that MFCs provided at least two orders of magnitude more surface area than round-bottom flasks, which could greatly improve the mass and heat transfer performance of chemical reactions. Two heat-transfer channels were designed sandwich like along two sides of the 3D mixing channel to carry liquid to ensure the reaction temperature (Fig. S2 in Supporting information). Thus, temperature, a key limitation in chemical processes,

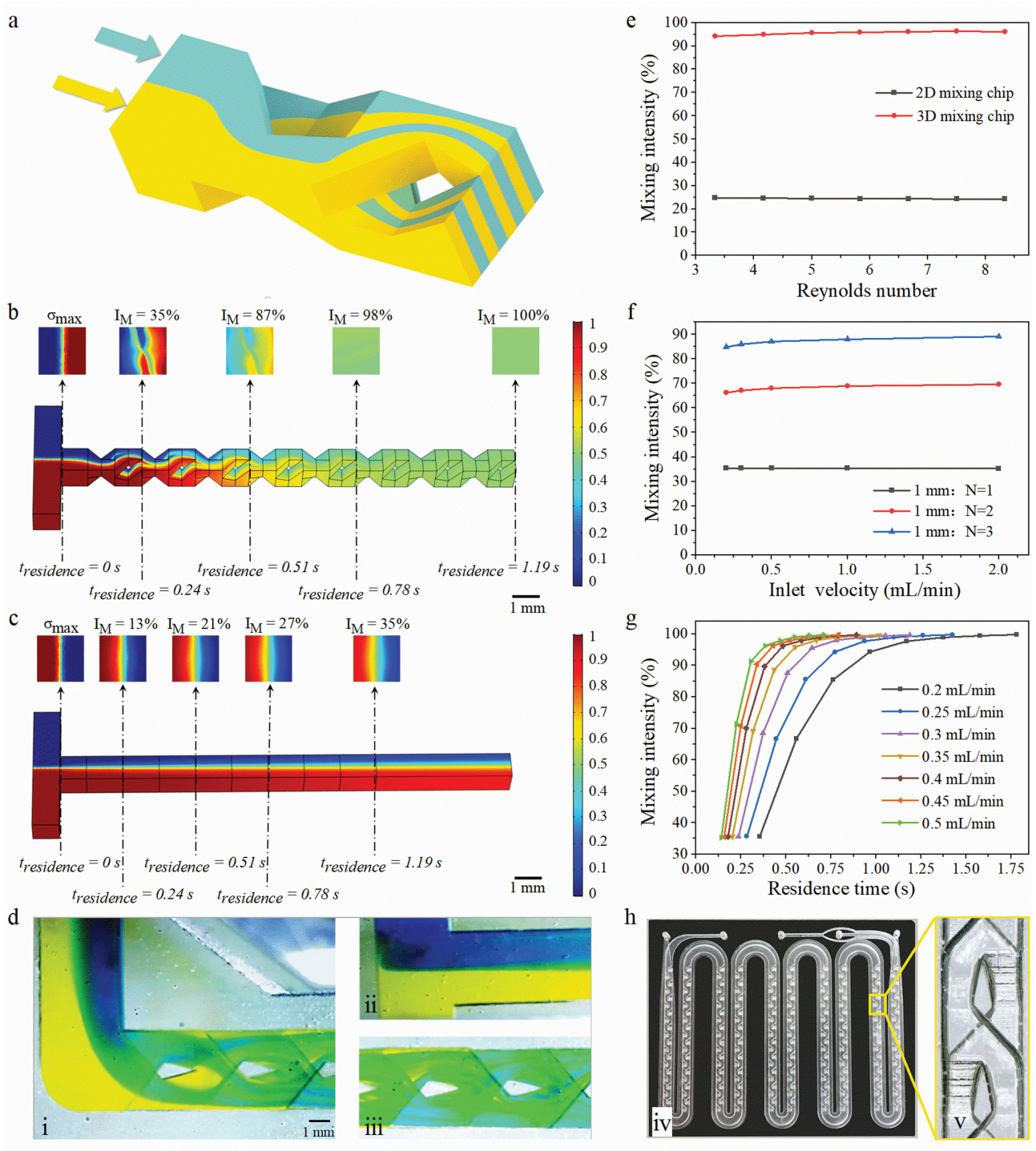

Fig. 1. Schematic view of (a) the microchip's 3D mixing units, (b) 3D mixing chip and (c) 2D mixing chip. Numerical simulations of mixing performances in a microchannel consisting of eight mixing units ($v = 0.3$ mL/min). Both of the two mixing channels adopted T-shaped inlet, and the inlet section size of the mixed flow channel was 1 mm × 1 mm. Red and blue represented molar concentration of fluids of 1 mol/L and 0 mol/L, respectively. Green color represented the two fluids were mixed completely and the molar concentration of fluid approached 0.5 mol/L. (d) (i) Microscope images of the mixing behaviors of the blue and yellow ink solutions in fabricated 3D micromixer ($v = 0.3$ mL/min), (ii) the detailed feature of the microfluidics chip's inlet, (iii) the detailed feature of the mixing units. (e) The mixing efficiency of 3D mixing chip and 2D mixing chip with the same liquid holding volume at low Reynolds number. (f) The mixing efficiency distribution in time and space of the 1 mm × 1 mm mixed flow channel in 3D mixing chip. N was the number of mixing units. (g) The relationship between residence time and mixing efficiency under different flow rates in 3D mixing chip with the 1 mm*1 mm mixed flow channel. (h) (iv) Photograph of the microfluidic chip. (v) the close-up view of the mixing units in position of yellow rectangle.

would be accurately regulated. Two types of 3D MFCs were designed based on the data above, a mixing chip and a reaction chip (Fig. 1h and Fig. S3 in Supporting information). Simulation of the reaction chip showed that the mixing efficiency was still high even with the expansion of channel size (Figs. S1 and S3 in Supporting information). The highly efficient 3D MFCs was well demonstrated, both experimentally and numerically, that could be used in applications ranging from chemical analysis and synthesis of materials to microreaction of fine chemistry.

Table 2
Comparison of the surface area per reactor volume between the batch and MFCs reactor.

Reactor type	Specific area, S/V (m^2/m^3)
MFC (1.6 mL)	9680
MFC (6.8 mL)	2510
MFC (10 mL)	2350
Round bottom flask (250 mL, half filled with liquid)	20

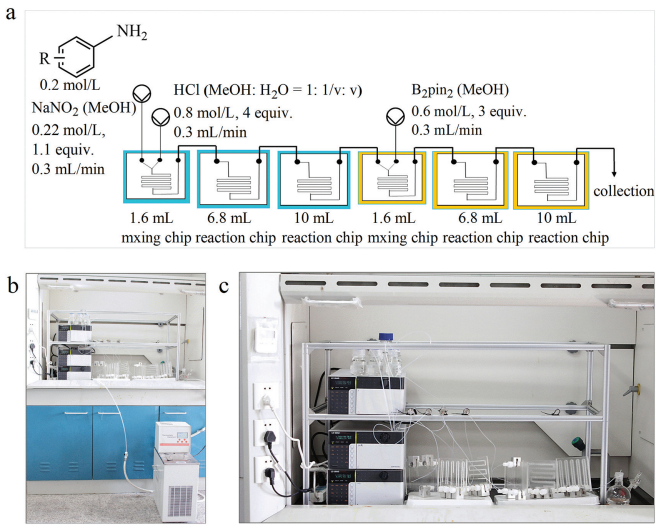

Fig. 2. (a) Processing continuous flow MFCs devices; (b, c) and photos regarding the setup for a flow MFCs study of aryl borates.

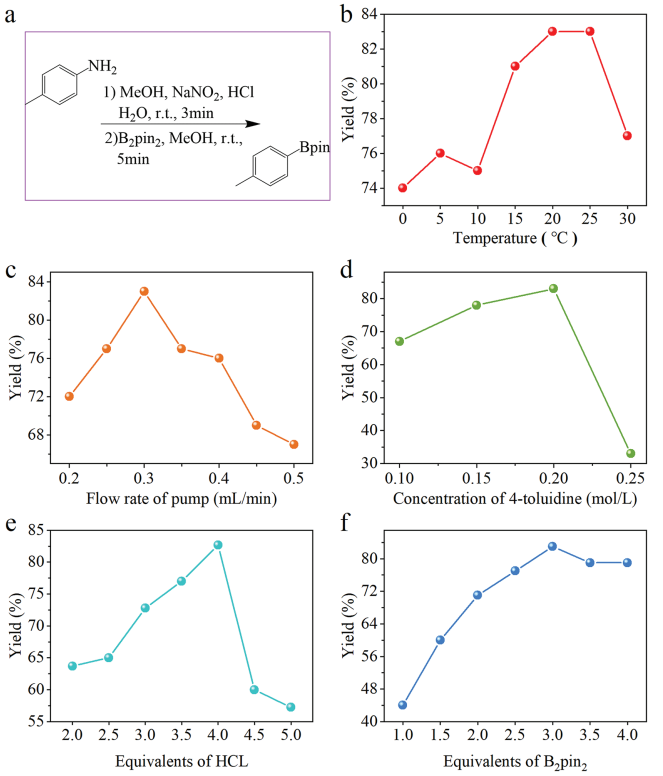

Fig. 3. (a) The coupling of 4-toluidine with bis(pinacolato)diboron. The effect of the parameters: (b) residence temperature for step 1, (c) flow rate of the pumps, (d) concentration of 4-toluidine, (e) equivalents of HCl, (f) amoount of B_2pin_2, based on the combination of MFCs of Table S1, entry 6.

Taking into account our goal and the benefits of our MFCs, such as precise temperature control and high-efficiency heat and mass transfer, we turn our attention to applying them to some beneficial reactions. Aryboronic acids and arylboronates are extensively capitalized as intermediates while synthesizing pharmaceutical and agrochemical materials [26–29]. Owing to their unique chemical-safety properties (high stability, low toxicity), such compounds are vital reagents during formations of carbon-carbon bonds and carbon-heteroatom bonds through Suzuki and other coupling reactions [30–32]. Moreover, the basic luminescence of arylboronates is only beginning to be realized, as evidenced by the recent discovery that phenyl-Bpins are capable of room-temperature phosphorescence in air [33]. So the development of fresh and fascinating uses for organoboron reagents will undoubtedly continue, and the constant need to increase chemical synthesis efficiency necessitates creativity [34]. Flow chemistry has increasingly been used to the large-scale synthesis of aryl boron reagent [35,36]. They lowered the flow reaction time to 50 min or 15 min, respectively, boosted the space-time yield by 50 or 30 times, and needed photoinitiation. It had also been reported to reduce the borylation time to less than 10 min, but it needed to be catalyzed with *n*–butyl lithium and carried out at ice bath [37]. The past decade has witnessed a renaissance of aryl diazonium chemistry and the Sandmeyer-type borylation of aryl diazonium salts for the production of aryl boronic acids and boronates has received a lot of attention [38]. Inspired by the previous report which provided an effective metal-free methanol-promoted borylation of arylamines [39], we proposed an *in situ* formation of aryldiazonium salts and subsequent borylation with bis(pinacolato)diboron in a continuous flow by MFCs for further optimization (Fig. 2a). Without using light, a free radical initiator, or transition metal catalysis, we were able to shorten the reaction time while also greatly increasing the space time yield at room temperature (Fig. 3a). The potential of femtosecond laser-tailored 3D MFCs as an efficient means for cost-effective synthesis was demonstrated by improving the reaction efficiency in this work.

In view of our previous experiments and related reports, the basic MFCs combination and experimental procedure were first implemented, aimed at screening the excellent range of operating conditions and scale-up. The continuous flow device used in this study for the synthesis of aryl borates was shown in Figs. 2b and c. In a previous study [39], methanol was regarded as solvent. To mitigate the precipitation of aryl diazonium salts and NaCl, combined solvent ($MeOH:H_2O = 1:1$, v:v) was applied instead of MeOH for the preparation of aryl diazonium salts.

The temperature for preparation of aryl diazonium salts in MFCs was then investigated in the range of 0–30 °C (Fig. 3b). Yields of the reaction performed under 20–25 °C showed no difference for short residence time. A further increase in temperature to 30 °C caused the decomposition of the diazonium salt. These results revealed that continuous flow MFCs devices could synthesize aryl diazonium salts safely and controllably at room temperature. With the optimized temperature conditions, the influence of pump flow rate on the reaction was investigated. Based on the mechanism of this reaction, equivalent ratios of all reactants were determined when the solution was prepared. The adjustment of the flow rate of each HPLC pump was consistent. As shown in Fig. 3c, 0.3 mL/min showed the best yield. The flow rate at 0.1–0.2 mL/min might be too slow to mix the reaction fluids while that at 0.4 mL/min might result in the lack of residence time. Once the previous several influencing factors had been optimized, the effect of changing reactant concentration on yield was considered. It was found that concentration of 0.25 mol/L would lead to insoluble solids which would trigger the system alarm (Fig. S6 in Supporting information). By adjusting the proportion of methanol in hydrochloric acid

Table 3
Comparison between the batch and MFCs reaction.

Parameters	Batch	MFCs
Temp. (°C)	0–5	25
T (min)	90	8
Yield (%)	74	95
Steps	Separated	Unseparated
Large scale	Hard to achieve	Easy to achieve
Safety	Potentially explosive	Inexplosive
Equivalent of HCl	6	4
STY (g h^{-1} L^{-1})	264.3	259,443.1

Table 4
Results for substituents' effect.

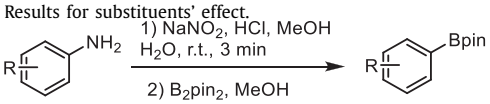

Entry	R	Product **2**	Batch yield (%)	Flow yield (%)
1	4-Me	**2a**	74	95
2	4-F	**2b**	54	87
3	4-NC	**2c**	57	55
4	2-Me	**2d**	45	48
5	3-COOH	**2e**	—	41

solvent, it could not solve the microchip blockage caused by insufficient solution of inorganic salt. Based on the trend showed in Fig. 3d, the concentration of 4-toluidine was determined to be 0.2 mol/L. In general, diazotization was carried out under highly acidic conditions. In addition to the formation of nitrite, excessive acid was mainly used to stabilize the diazonium salt. Seven experiments were conducted by changing the equivalents of HCl, the yield changes in MFCs were investigated (Fig. 3e). The results showed that an excellent yield was obtained while 4 equiv. of HCl were applied. However, if the acid concentration continued to increase, the concentration of free amine would decrease, and therefore, slow down the rate of diazotization. Further optimization was focused on the amount of B_2pin_2. The use of 3 equiv. of B_2pin_2 would results in best yield. Yet, more or less B_2pin_2 could not give positive influences.

By virtue of the residence time required by chemical reaction, the original reaction chips with large liquid volume were designed to optimize reactive conditions. For the first attempt at MFCs combination, only 53% yield was obtained when the reaction was conducted at 25 °C with residence time for 50 min (entry 1, Table S1 in Supporting information). After different combinations of MFCs were explored (Table S1), the MFCs combination with the highest yield performance (83%) was determined (Table S1, entry 6). However, longer reaction time in the first step resulted in poor yield probably due to the decomposition of the diazotization salt (Table S1, entry 7). It was also proved that increasing the reaction time was essential for the borylation of aryldiazonium salts (Table S1, entries 4 and 6). But excessively prolonging the residence time of the second step did not significantly improve the yield of the reaction. Meanwhile, it was found that the reactants could not fill the reaction channel perfectly under low flow rate, and mass transfer was still very important in the reaction process. On the contrary, adequate residence time mass transfer would sacrifice effect, which would degrade the ultimate yield and reaction time. Therefore, a brand-new chip was designed, and the channel size of which was the same as previous hybrid chip, while the maximum liquid holding volume (2.7 mL) could be processed under the same chip area (Fig. S3). After applying the previous screening conditions, 95% yield and 8 min reaction time were obtained (Table S1, entry 11).

To highlight the advantages of the MFCs, the comparison with the reaction in batch was summarized in Table 3. The use of MFCs chemical processes with high yield required less corrosive reagent consumption. The reaction temperature was changed from ice bath to room temperature and the residence time was cut by 10 times to greatly save energy. It was noted that the method leads to significant simplification of reaction processes and equipment, shorter production cycles, savings in most human costs and improved safety performance. Specifically, the space time yield of MFCs was 982 times higher than batch reaction (Space time yield (STY): $STY_{MFCs} = 259{,}443.1\ g\ h^{-1}\ L^{-1}$; $STY_{batch} = 264.3\ g\ h^{-1}\ L^{-1}$).

With the optimized reaction condition in hand, the tolerance of different functional groups at the aromatic ring was subsequently explored (Table 4). A variety of substrates were subjected to aryl borate ester formation with good conversion to the corresponding cross coupling products yields of 41%–95%. Especially, synthetic intermediate **2b** which could be turned into a treatment for diabetes was successfully obtained with higher yield compared to traditional batch process [40]. Meanwhile, **2e**, which could be converted into a drug intermediate for the treatment for idiopathic thrombocytopenic purpura (ITP) [41], was obtained with moderate yield. Some specific substituent groups, such as **2d**, the 24 h synthesis yield was only 40% in another experiment [42]. For **1c**, this substrate was provided bad conversion to the desired products in previous flow chemistry study and consequently required significant manual handling in order to purify the material [43]. The reaction time was substantially reduced to 8 min and the space time yield was greatly enhanced while ensuring the original yields of **2c** and **2d** in this work. The study firstly proposed the considerable significance of the range of parameters (MFCs combination, reaction temperature, flow rate, concentration) which could quantitatively influence the yield of diazonium salt in the MFCs, and therefore, determine the subsequent multistep reactions.

In summary, we have designed innovative 3D MFCs using ultrafast laser micromachining which can realize efficient mixing in different centimeter-level 3D channel for chemical synthesis. It embodies our equipment's operational miniaturization, high integration in chemical applications, and the fact that our equipment takes up less space, poses fewer leaks, and saves a huge amount of resources. Surprisingly, our technique is far less expensive than existing photolithography and glass mask technologies on the market, and the custom cycle is short, allowing us to respond rapidly to customer needs. Taking arylborate esters as an example, a new, simplified, time-saving, economical and hazardless flow synthetic protocol was developed for organic synthesis *via* MFCs. The newly developed catalyst-free system which synthesized and consumed aryl diazonium salts safely and controllably at room temperature *in situ* has obvious advantages in terms of ease of scale-up, fast reaction and absence of metal contamination. Further application of this technology in the field of drug synthesis will be explored in future publications.

Declaration of competing interest

The authors declare that they have no known competing financial interests or personal relationships that could have appeared to influence the work reported in this paper.

Acknowledgment

This work was supported by the Shanghai Municipal Science and Technology Major Project ("Beyond Limits manufacture").

Supplementary materials

Supplementary material associated with this article can be found, in the online version, at doi:doi:10.1016/j.cclet.2022.07.037.

References

[1] A.P. Mattey, G.J. Ford, J. Citoler, et al., Angew. Chem. Int. Ed. 60 (2021) 18660–18665.
[2] J. Wegner, S. Ceylan, A. Kirschning, Chem. Commun. 47 (2011) 4583–4592.
[3] C.A. Shukla, A.A. Kulkarni, Beilstein J. Org. Chem. 13 (2017) 960–987.
[4] R.L. Hartman, J.P. McMullen, K.F. Jensen, Angew. Chem. Int. Ed. 50 (2011) 7502–7519.
[5] L. Huck, A. de la Hoz, A. Diaz-Ortiz, J. Alcazar, Org. Lett. 19 (2017) 3747–3750.
[6] I. Rossetti, Catal. Today 308 (2018) 20–31.
[7] K. Geyer, J.D. Codee, P.H. Seeberger, Chem. Eur. J. 12 (2006) 8434–8442.
[8] A. Gholamipour-Shirazi, C. Rolando, Org. Process Res. Dev. 16 (2012) 811–818.
[9] H. Becker, L.E. Locascio, Talanta 56 (2002) 267–287.
[10] J.N. Lee, C. Park, G.M. Whitesides, Anal. Chem. 75 (2003) 6544–6554.
[11] F. Liang, Y. Qiao, M. Duan, et al., RSC Adv. 8 (2018) 8732–8738.
[12] P. Domachuk, K. Tsioris, F.G. Omenetto, D.L. Kaplan, Adv. Mater. 22 (2010) 249–260.
[13] G.M. Whitesides, Nature 442 (2006) 368–373.
[14] S.K. Piendl, T. Schönfelder, M. Polack, et al., Lab Chip 21 (2021) 2614–2624.
[15] W. Wang, S. Zhao, T. Shao, Y. Jin, Y. Cheng, Chem. Eng. J. 192 (2012) 252–261.
[16] M. Nimafar, V. Viktorov, M. Martinelli, Chem. Eng. Sci. 76 (2012) 37–44.
[17] T. Yasui, Y. Omoto, K. Osato, et al., Lab Chip 11 (2011) 3356–3360.
[18] R.R. Gattass, E. Mazur, Nat. Photonics 2 (2008) 219–225.
[19] Y. Cheng, K. Sugioka, K. Midorikawa, Opt. Lett. 29 (2004) 2007–2009.
[20] Y. Hanada, K. Sugioka, H. Kawano, et al., Biomed. Microdevices 10 (2008) 403–410.
[21] Y. Hanada, K. Sugioka, I.S. Ishikawa, et al., Lab Chip 11 (2011) 2109–2115.
[22] Y. Liao, J. Song, E. Li, et al., Lab Chip 12 (2012) 746–749.
[23] J. Qi, W. Li, W. Chu, et al., Micromachines 11 (2020) 213.
[24] P. Carrière, Phys. Fluids 19 (2007) 118110.
[25] X. Ren, C. Shen, G. Wang, et al., Org. Lett. 23 (2021) 2527–2532.
[26] D. Qiu, L. Jin, Z. Zheng, et al., J. Org. Chem. 78 (2013) 1923–1933.
[27] M.P. Silva, L. Saraiva, M. Pinto, M.E. Sousa, Molecules 25 (2020) 4323.
[28] J Takaya, N Iwasawa, ACS Catal. 2 (2012) 1993–2006.
[29] C.T. Yang, Z.Q. Zhang, Y.C. Liu, L. Liu, Angew. Chem. Int. Ed. 50 (2011) 3904–3907.
[30] J.J. Dai, W.M. Zhang, Y.J. Shu, et al., Chem. Commun. 52 (2016) 6793–6796.
[31] D.G. Hall, Chem. Soc. Rev. 48 (2019) 3475–3496.
[32] B. Akgun, D.G. Hall, Angew. Chem. Int. Ed. 57 (2018) 13028–13044.
[33] H.E. Hackney, D.G. Hall, ChemPhotoChem (2022) e202100219.
[34] J.W.B. Fyfe, A.J.B. Watson, Chem 3 (2017) 31–55.
[35] F. Lima, M.A. Kabeshov, D.N. Tran, et al., Angew. Chem. Int. Ed. 55 (2016) 14085–14089.
[36] K. Chen, S. Zhang, P. He, P. Li, Chem. Sci. 7 (2016) 3676–3680.
[37] Y. Takahashi, Y. Ashikari, M. Takumi, et al., Eur. J. Org. Chem. 2020 (2020) 618–622.
[38] F. Mo, D. Qiu, L. Zhang, J. Wang, Chem. Rev. 121 (2021) 5741–5829.
[39] D. Xue, C.J. Zhao, Z.H. Jia, C. Wang, J. Xiao, Synlett 25 (2014) 1577–1584.
[40] A.K.L. Yuen, C.A. Hutton, Tetrahedron Lett. 46 (2005) 7899–7903.
[41] S.P.A. Hinkes, C.D.P. Klein, Org. Lett. 21 (2019) 3048–3052.
[42] N. Miralles, R.M. Romero, E. Fernández, et al., Chem. Commun. 51 (2015) 14068–14071.
[43] J.A. Newby, L. Huck, D.W. Blaylock, et al., Chem. Eur. J. 20 (2014) 263–271.